JOURNAL OF OPTOELECTRONICS AND ADVANCED MATERIALS, Vol. 12, No. 5, May 2010, p. 1024 - 1029

Optical band gap and Raman spectra in $A_xB_{0.2-x}(TeO_2)_{0.8}$ glasses

J. OZDANOVA, H. TICHA, L. TICHY[a*]
Faculty of Chemical Technology, University of Pardubice, 532 10 Pardubice, Czech Republic
[a]Institute of Macromolecular Chemistry of the Academy of Sciences of the Czech Republic v.v.i., Heyrovsky sq. 2, 120 06 Prague, Czech Republic, Present address: Joint Laboratory of Solid State Chemistry of Institute of Macromolecular Chemistry of the Academy of Sciences of the Czech Republic v.v.i. and the University of Pardubice, 532 10 Pardubice, Czech Republic

Seven different glasses with the molar fraction of TeO_2 equal to eighty were prepared from pure oxides. The optical band gap was determined in the region 3.33 - 3.61 eV. The coefficient of the temperature dependence of the optical band gap was found in the region 3.8×10^{-4} - 6.8×10^{-4} eVK^{-1}. From the optical band gap the non-linear refractive index value of the studied glasses was estimated at around 0.85×10^{-11} esu. Reduced Raman scattering spectra indicate structural changes induced, by chemical composition, in TeO_2 network due to conversion from TeO_4 trigonal bipyramids to TeO_3 and TeO_{3+1} units. A qualitative correlation in $TeO_4 \rightarrow TeO_3$ and TeO_{3+1} conversion and the optical band gap was found.

(Received May 6, 2010; accepted May 26, 2010)

Keywords: Tellurite glasses, Optical band gap, Raman scattering

1. Introduction

Tellurite glasses have high polarizabilities, high Raman scattering cross sections and in infrared region they are transparent up to 7 μm [1, 2]. Higher laser damage resistance of tellurite glasses, in comparison with chalcogenide glasses, allows use of high intensity laser pumping to reach high non-linear optical effects [4].

Recently the influence of various oxides as modifiers on the structural network and some optical properties of tellurite glasses were examined [3-5]. For binary glasses $(M_nO_m)_x(TeO_2)_{1-x}$ where M = Ti, Nb the compositional invariance of the Raman spectra has been interpreted as a kind of structural conservatism because similarity of Te-O and M-O force constants. It is suggested that namely the atoms with valences IV and V and certain atoms with valences III can not change significantly the potential wells of oxygen atoms and hence the Raman spectra are nearly invariant to the chemical composition while in $(Tl_2O)_x(TeO_2)_{1-x}$ glassy system Tl_2O behaves as a strong modifier due to forming of island-type Tl_2TeO_3 structure [3]. Five different binary glasses with the chemical composition $(M_nO_m)_{15}(TeO_2)_{85}$, where M = W, Ti, Nb, Pb, Ga were studied in relation to the influence of a modifier on the physical properties of tellurite glasses with constant molar fraction of TeO_2. It was shown that the thermal stability increases with addition of the oxides of d^0 elements (oxides of W^{6+}, Ti^{4+}, Nb^{5+}) and "the TeO_2 network structure varies for d^{10}, ns^2 (Pb^{2+}) and d^0 species (Ga^{3+})". The results obtained indicate a strong influence of the specific oxide modifier on the Raman vibration related to TeO_3 (trigonal pyramid) structural unit. The glasses where M = Ti, Nb are suggested to be promising candidates for applications based on a discrete Raman amplification [4]. The role of modification of Tl_2O - TeO_2 glasses by TiO_2 (5 mol%), ZnO (10 mol%), Ga_2O_3 (10 mol%), PbO(5 mol%) and Bi_2O_3 (5 mol%), where the ratio of Tl_2O/TeO_2, in molar fraction, varied from 28.5/66.5 for modification by PbO to 38/57 for modification by Bi_2O_3, was examined in relation to the changes in the third - order nonlinear optical susceptibility and structural changes reflected in the Raman scattering [5]. Except of modification by Ga_2O_3 in all cases the most intensive Raman feature was observed at around 690-725 cm^{-1} attributed to presence of isolated $[TeO_3]^{2-}$ anions. However, contrary to all other modifiers the modification by TiO_2 favors network polymerization as indicated by highest glass-transition value (T_g = 209 ºC) and high intensity of the broad Raman feature at around 450 cm^{-1} belonging to covalently bonded Te-O-Te, Te-O-M and M-O-M bridges. Just the network polymerization is suggested to be responsible for highest third-order susceptibilities for $5TiO_2$-$30TlO_{1.5}$-$65TeO_2$ glass [5].

In this communication some our recent results [6-8] and new results related to $A_xB_{0.2-x}(TeO_2)_{0.8}$ glasses, where for $0.2 > x > 0$: A = Li_2O or BaO and B = TiO_2, A = PbO or ZnO and B = Nb_2O_5 and Bi_2O_3 and for x = 0: B = Nb_2O_5 or PbO, namely to the optical band gap and structural arrangement deduced from Raman scattering measurements are summarized. We restricted our study on the glasses with constant molar fraction of TeO_2 equal to 80% in order to reduce possible role of TeO_2 content on the structural arrangement of the glasses considered.

2. Experimental

Glasses examined in the presented study (see Table 1 for overview), were prepared from corresponding oxides PbO, Nb_2O_5, ZnO, TeO_2 and from Li_2CO_3 and $Ba(NO_3)_2$ (purity 99.95 %, Sigma Aldrich) as described in Refs. [6-8]. The chemical composition was verified employing X-ray diffraction analysis (JEOL JSM 5500 LV, Japan). The density of the bulk glasses (5g sample) was measured by Archimedean method in the distilled water. The values of the dilatometric glass-transition temperature (T_g) and the coefficient of thermal expansion were determined as described in Ref. [9].

Optical transmission in UV-VIS spectral region was measured on the samples prepared by a glass blowing. The samples with the thickness (d) varying in the region 1 μm ≤ d ≤ 7 μm were used. Some details of the optical transmission (T) and reflectivity (R) measurements were described recently [10]. Optical band gap values (E_g) for the samples involved within this study were determined assuming non-direct optical transitions from the relation: $(Kh\nu)^{1/2} = B^{1/2}(h\nu-E_{g,non})$, where $E_{g,non}$ is the non-direct optical band gap, $B^{1/2}$ the slope of the short wavelength absorption edge (SWAE) reflects the sample disorder [11], hν is the photon energy, and K is the absorption coefficient calculated using the relation $K = (1/d)\ln\{[(1-R)^2+((1-R)^4+4R^2T^2)^{1/2}]/2T\}$, [12].

Raman spectra were recorded using FTIR spectrometer Bruker model IFS 55 equipped with FRA 106 Raman module in back scattering geometry using a Nd:YAG laser beam (excitation light wavelength λ = 1064 nm, slit width 4 cm^{-1}, laser power ≈ 300 mW at the sample surface). All Raman spectra were taken at room temperature in the spectral region 50 - 1000 cm^{-1} using 200 scans of the bulk sample with a flat optical surface. The Bose-Einstein correction has been applied to the spontaneous Raman scattering data

3. Results

The chemical composition of studied glasses, their density values (ρ), the formal volume fraction of TeO_2 (f.v.f.), the dilatometric glass-transition temperature (T_g) and the coefficient of thermal expansion (α) are summarized in Table 1.

The density values were calculated using the relation $\rho_{(x)} = \sum x_i M_i / \sum x_i V_{Mi}$ where x_i, M_i and V_{Mi} ($=M_i/\rho_i$) are the molar fraction, the average molar weight, average molar volume and the density of an i-th component of a glass, respectively. Following values of the density, in gcm^{-3}, were used: $\rho_{(Li2O)} = 2.01$, $\rho_{(TiO2)} = 3.9$, $\rho_{(BaO)} = 5.72$, $\rho_{(Nb2O5)} = 4.47$, $\rho_{(PbO)} = 9.53$, $\rho_{(ZnO)} = 5.61$, $\rho_{(Bi2O3)} = 8.9$. The formal volume fraction of TeO_2 was estimated using the relation: $f.v.f. = 0.8 \times V_{M\,(TeO2)} / \sum x_i V_{Mi}$. There is quite good agreement between experimental and calculated density values, the error = $100 \times (\rho_{exp} - \rho_{calc}) / \rho_{exp}$ varies from -0.2 to -3.6 %.

Table 1. The chemical composition expressed as $A_xB_{0.2-x}$ of $A_xB_{0.2-x}(TeO_2)_{0.8}$ glasses, the values of experimental (exp) and calculated (calc) density, in gcm^{-3}, the formal volume fraction of TeO_2, the dilatometric glass transition temperature, in °C and the coefficient of thermal expansion , in $ppmK^{-1}$, of the studied glasses.

Chemical Composition	ρ,exp	ρ,calc	TeO_2 f.v.f.	T_g	α
$(Li_2O)_{0.1}(TiO_2)_{0.1}$	5.13_8	5.32	0.86_4	317	19
$(Li_2O)_{0.15}(TiO_2)_{0.05}$	5.09_7	5.22_6	0.86_4	287	/
$(BaO)_{0.1}(TiO_2)_{0.1}$	5.45_2	5.54_2	0.86_4	287	18
$(Nb_2O_5)_{0.2}$	5.24	5.25_5	0.65_4	411	11
$(PbO)_{0.1}(Nb_2O_5)_{0.1}$	5.72	5.73_2	0.73_1	358	15
$(PbO)_{0.2}$	6.27	6.33_5	0.82_8	281	21
$(ZnO)_{0.15}(Bi_2O_3)_{0.05}$	5.88_2	5.97_5	0.82_4	321	20

Except of the glasses with Nb_2O_5 also the f.v.f. of TeO_2 is remains to be comparable.

Typical spectral dependencies of the optical transmission are shown in Fig. 1.

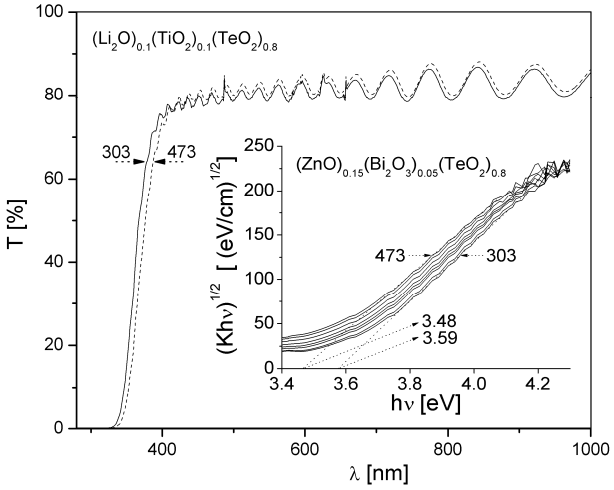

Fig. 1. Spectral dependencies of the optical transmission at two temperatures, 303 and 473 K, for the samples prepared by blowing of glass. In the inset spectral dependencies of the absorption coefficient at various temperatures are shown assuming non-direct optical transition [11]. The dotted lines fit to relation $(Kh\nu)^{1/2} = B^{1/2}(h\nu-E_{g,non})$.

The temperature dependencies of the optical band gap $E_{g,non}(T)$ approximated by relation $E_{g,non}(T) = E_{g,non}(0) - \gamma T$ are shown in Fig.2. The room temperature values of the optical band gap and the coefficient of the temperature dependence of the optical band gap (γ) are summarized in Table 2.

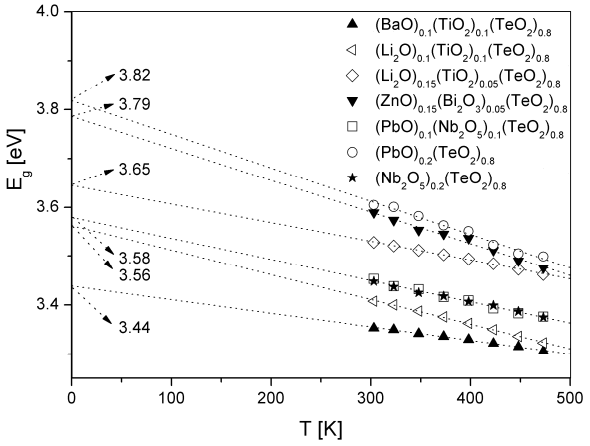

Fig. 2 Temperature dependencies of the optical band gap ($E_{g,non}$). Dotted lines fit to relation: $E_{g,non}(T) = E_{g,non}(0)-\gamma T$. The numbers indicate the extrapolated values of $E_{g,non}(T\rightarrow 0)$.

Table 2. The chemical composition expressed as $A_xB_{0.2-x}$ of $A_xB_{0.2-x}(TeO_2)_{0.8}$ glasses, the optical band gap ($E_{g,non}$) in eV, the coefficient of the temperature dependence of the optical band gap (γ) in eVK^{-1} and the non-linear refractive index (n_2) in esu estimated from the optical band gap. The values of non-linear refractive index were estimated using the relation: $n_2 \approx 1.26\times10^{-9}/(E_{g,non})^4$ [13].

Chemical composition	$E_{g,non}$	$\gamma\times10^{-4}$	$n_2\times10^{-11}$
$(Li_2O)_{0.1}(TiO_2)_{0.1}$	3.41	5.3	≈0.9
$(Li_2O)_{0.15}(TiO_2)_{0.05}$	3.53	3.8	≈0.8
$(BaO)_{0.1}(TiO_2)_{0.1}$	3.33	5.9	≈1
$(Nb_2O_5)_{0.2}$	3.45	4.3	≈0.9
$(PbO)_{0.1}(Nb_2O_5)_{0.1}$	3.45	4.3	≈0.9
$(PbO)_{0.2}$	3.61	6.8	≈0.74
$(ZnO)_{0.15}(Bi_2O_3)_{0.05}$	3.58	6.5	≈0.77

In Figs. 3 and 4 Raman spectra for A_x $(TiO_2)_{0.2-x}(TeO_2)_{0.8}$ glasses (Fig.3) and for heavy metal oxide (HMO) glasses (Fig.4) are shown. The spectra were decomposed using standard Opus 3.0 software (Bruker) assuming that Raman Feature (RF) in the wavenumber region 600 - 900 cm^{-1} and 300 – 600 cm^{-1} reflects mainly Raman activity of TeO_2 based part of a network. Hence in considered wavenumber regions we decomposed corrected Raman spectra into six distinct RF [14] (marked A, A´, B, C, D, E in Figs.3 and 4). For the glasses containing Nb_2O_5 the additional new RF (RF_F) at around 890 cm^{-1} appeared. We note that the fit in the region 50 - 300 cm^{-1} should be taken with a care due to an uncertainty related to a number of the oscillators (for various numbers of oscillators the quality of more fits was comparable).

Depending on the chemical composition RF obtained by decomposition are in the following wavenumber region: RF_A in 412 - 453 cm^{-1}, $RF_{A'}$ in 485 - 511 cm^{-1}, RF_B in 593 - 623 cm^{-1}, RF_C in 650 - 663 cm^{-1}, RF_D in 715 - 738 cm^{-1}, RF_E in 769 - 804 cm^{-1} and RF_F in 883 - 898 cm^{-1}. Observed RF can also be classified according to Refs. [15-17] as it follows: (α) RF due to "acoustic Raman" (RF_{AC}), typically observed in the region $\nu \approx 50$ - 100 cm^{-1}. This low frequency Raman feature could, however, be also assigned to Boson peak reflecting an excess of low-frequency vibrational states as discussed for instance in Refs. [18, 19]. (β) RF due to a motion of heavy metal ions (RF_{HM}) observed in the region $\nu \approx 70$ - 160 cm^{-1}. (γ) RF observed in the region $\nu \approx 360$ - 600 cm^{-1} due to "bridged-anion" (RF_{BA}) that is due to symmetric stretch motion of oxygen in C-O-C bridge (C represents cation) and (δ) RF observed in the region $\nu \approx 650$ - 950 cm^{-1} due to "non-bridged-anion" (RF_{NBA}) that is due to asymmetric C_1--O-C_2 bridge with C_1--O bond sufficiently longer than that one of C_2-O bond. The other origin of RF_{NBA} suggested is the C-O^- configuration [17]. From Figs.3 and 4 it is clear that the most evident differences in Raman scattering are following:

(i) For the glasses with the chemical composition $(PbO)_{0.2}$ $(TeO_2)_{0.8}$ and $(ZnO)_{0.15}Bi_2O_3)_{0.05}(TeO_2)_{0.8}$ glasses the intensity (I) of RF_D exceeds the intensity of RF_C ($I(RF_C) > I(RF_D)$). (ii) For the glass $(Nb_2O_5)_{0.2}(TeO_2)_{0.8}$ well pronounced RF is observed at around 235 cm^{-1}, see Fig.4. (iii) For the glass $(PbO)_{0.2}$ $(TeO_2)_{0.8}$ the Raman activity of RF_A and $RF_{A'}$ seems to decreased in comparison with Raman activity of RF_A and $RF_{A'}$ in other considered glasses. (iv) For the glasses containing Nb_2O_5 new well resolved RF appeared at around 890 cm^{-1}, Fig.4.

4. Discussion

We shall restrict our discussion to the wavenumber region 300 – 900 cm^{-1} where the most important Raman features related to the Raman activity of TeO_2 based networks are present. Following Ref. [20] the individual RF in the wavenumber region 600-900 cm^{-1} we assign as follows:

≈ 610 cm^{-1} ↔ RF_B to antisymmetric stretching of TeO_4 trigonal bipyramids (tbp) forming a continuous network,

≈ 660 cm^{-1} ↔ RF_C to antisymmetric vibration of Te-O--Te linkages formed by two nonequivalent Te-O bonds

and its intensity reflects both the density of TeO_4 tbp but also a degree of distortion of tbp units,

≈ 725 cm^{-1} ↔ RF_D to stretching modes of Te-O^- and Te=O bonds in TeO_3 trigonal pyramids (tp) or TeO_{3+1} polyhedra,

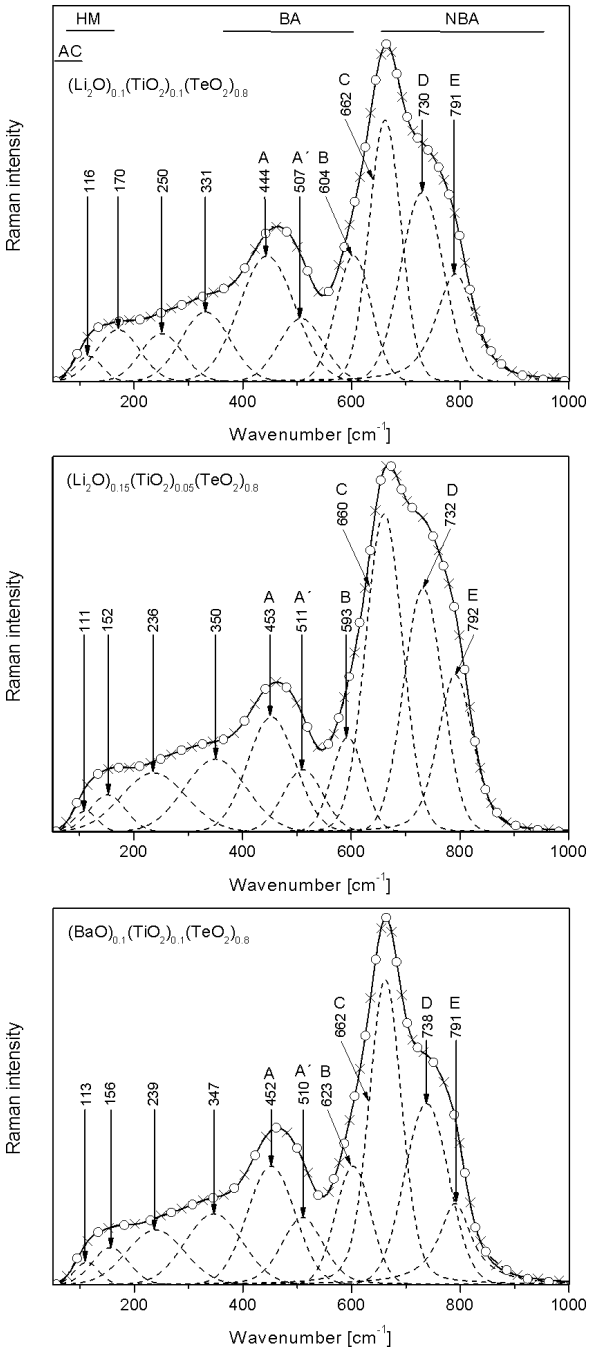

Fig. 3 Three Raman spectra of A_x $(TiO_2)_{20-x}(TeO_2)_{80}$ glasses. Dashed curves indicate the individual Raman features obtained by decomposition of the corrected spectra. The full curves marked by the crosses indicate corresponding envelopes; the corrected spectra are displayed by the dash-dotted curves marked by the open circles. The numbers indicate the peak wavenumber and the letters mark some most typical Raman features. The horizontal lines indicate the spectral region of Raman activity belonging to acoustic Raman features (AC) [15 - 17] or to Boson peak [18, 19], heavy – metal ions motion (HM), bridged – anion modes (BA) and non – bridged anion modes (NBA) [15-17].

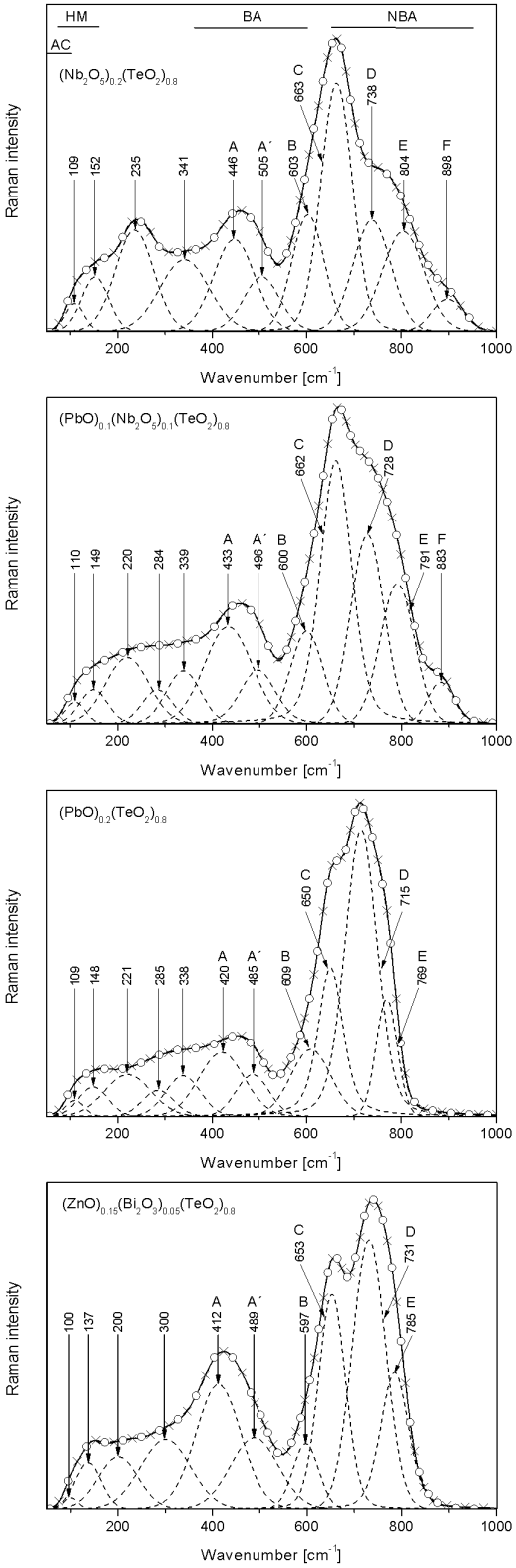

Fig. 4. Four Raman spectra of binary and ternary HMO - $(TeO_2)_{80}$ glasses. The curves, symbols, letters and the numbers have the same meaning as in Fig.1.

≈ 785 cm^{-1} ↔ RF_E to stretching modes of deformed TeO_{3+1} units and stretching motion of Te atoms bonded to non-bridging oxygen in TeO_3 tp.

Hence the RF_B and RF_C can be taken as a measure of Raman activity of TeO_4 structural units while RF_D and RF_E can be taken as a measure of Raman activity of TeO_3 structural units.

In the wavenumber region at around 400-500 cm^{-1} the broad band composed at least by two individual Raman features RF_A (≈ 440 cm^{-1}) and $RF_{A'}$ (≈ 500 cm^{-1}) is assigned to symmetrical stretching or bending vibrations of Te-O-Te, O-Te-O, Te-O-A,B linkages. It means that Raman activity in this region reflects a degree of polymerization of the network and diminishing of this band means a decrease of the network connectivity [5, 20].

In two glasses containing Nb_2O_5 the RF_F at around 890 cm^{-1} is assigned to vibration of isolated NbO_6 octahedra which could be distorted having one terminal (non-bridging) Nb-O bond [21] and the RF at around 235 cm^{-1} (RF_{235}) for $(Nb_2O_5)_{0.2}(TeO_2)_{0.8}$ glass belongs to bending vibration of Nb-O-Nb linkage [22]. Its presence indicates that some NbO_6 octahedra are connected. In such case the NbO_6 octahedra assist to polymerization which together with rather high bond energy of Nb-O bond (≈ 770 kJ/mol) contrary to energy of Te-O bond ≈ 376 kJ/mol [23] should lead to an increase in T_g as we observed, Table 1.

From the results displayed in Figs. 3,4 it is evident that overall Raman response of studied glasses is affected by the "modifiers" A_mO_n and/or B_mO_n oxides. For the first group (I.G) of studied tellurite glasses $((Li_2O)_{0.1}(TiO_2)_{0.1}$, $(Li_2O)_{0.15}(TiO_2)_{0.05}$, $(BaO)_{0.1}(TiO_2)_{0.1}$, $(Nb_2O_5)_{0.2}$, $(PbO)_{0.1}(Nb_2O_5)_{0.1})$ it is valid: $I(RF_C) > I(RF_D)$ which is an indication that in formation of TeO_2 based network the role of TeO_4 tbp exceeds the role of TeO_3 and or TeO_{3+1} units. For the second group of glasses (II.G) ($(PbO)_{0.2}$, $(ZnO)_{0.15}(Bi_2O_3)_{0.05}$): $I(RF_D) > I(RF_C)$ hence in this case the role TeO_3 and or TeO_{3+1} units in TeO_2 based network formation is more important. According to ab-initio molecular orbital calculations [24, 25] the difference between homo- and lumo-states is lower for TeO_4 tbp unit whereas it is higher in the case of tp TeO_3 and TeO_{3+1} unit. It means that the optical band gap should increase for the glasses where a role of TeO_3 and or TeO_{3+1}, in the network formation exceeds, the role of TeO_4 units. Therefore we adopt the ratio $r = [A(RF_D) + Ar(RF_E)]/[Ar(RF_B) + Ar(RF_C)]$, where $Ar(RF_X)$ is the area of the corresponding Raman feature, for a qualitative correlation between structural changes and optical band gap changes. We found that r = 0.76, **1.08**, 0.76, 0.74, 0.99, **2.33**, **1.63** for E_g = 3.41, **3.53**, 3.35, 3.45, 3.45, **3.61**, **3.58** eV. That is higher values of r – more important role of TeO_3 and or TeO_{3+1} units in TeO_2 network formation and optical band increases as indicated by bold numbers. Because $I(RF_C)$ and consequently $Ar(RF_C)$ can be also affected by a degree of distortion of TeO_4 tbp units we used as an alternative measure $TeO_4 \rightarrow TeO_{3+1}$, TeO_3 conversion the another ratio $r,a = [I(RF_D) + I(RF_E)]/ I(RF_B)$, where $I(RF_X)$ is the Raman intensity of corresponding individual RF. In this case r,a varies in the region 1.95-6.15 and we obtained simple linear correlation between E_g and r,s: $E_g = 3.28 + 0.052\times$ r,s with $R_{sq} = 0.95$.

In Ref. [5] it was suggested that the ratio (ξ) of the band intensities, in our notation: $[I(RF_A) + I(RF_{A'})]/$ $[I(RF_B) + I(RF_C) + I(RF_D) + I(RF_E)]$ relates to the degree of polymerization and indeed for studied Tl_2O-TeO_2 glasses modified by Ti, Zn, Ga, Pb, Bi oxides the T_g values decrease with decrease in the ratio ξ. In the case of our glasses such one to one correlation between ξ and T_g is not observed. The values of ξ for our glasses were found to be equal to **0.341**, 0.21, **0.281**, 0.266, 0.216, 0.194, and **0.287** for T_g= **317**, 287, **355**, 411, 358, 281 and **321** °C, respectively. The numbers in bold mark the values of ξ and T_g for the glasses $(Li_2O)_{0.1}(TiO_2)_{0.1}(TeO_2)_{0.8}$, $(BaO)_{0.1}(TiO_2)_{0.1}(TeO_2)_{0.8}$, $(ZnO)_{0.15}(Bi_2O_3)_{0.05}(TeO_2)_{0.8}$ which owing rather high values of ξ do not follow even qualitative ξ (T_g) correlation. We speculate that possible reasons for rather higher values of ξ of those glasses could be following: (i) Formation of $TiTe_3O_8$ structural units which may assist to Raman activity in the wave number region 412 - 511 cm^{-1} because the Raman response of crystalline $TiTe_3O_8$ is observed at around 460 cm^{-1} [26]. (ii) Presence of ZnO like amorphous entities of which Raman activity is suggested to appear at around 600 cm^{-1} [27] and/or presence of ZnTeO and $Zn_2Te_3O_8$ structural units of which Raman activity may also be observed in considered wavenumber region [28].

5. Conclusions

In this communication we compared the changes in the reduced Raman spectra, in the optical band gap and in the glass-transition temperature of following glasses: $(Li_2O)_{0.1}(TiO_2)_{0.1}(TeO_2)_{0.8}$; $(Li_2O)_{0.15}(TiO_2)_{0.05}(TeO_2)_{0.8}$; $(BaO)_{0.1}(TiO_2)_{0.1}(TeO_2)_{0.8}$; $(Nb_2O_5)_{0.2}(TeO_2)_{0.8}$; $(PbO)_{0.1}(Nb_2O_5)_{0.1}(TeO_2)_{0.8}$; $(PbO)_{0.2}(TeO_2)_{0.8}$ and $(ZnO)_{0.15}(Bi_2O_3)_{0.05}(TeO_2)_{0.8}$.

We found that the changes in the chemical composition induce some structural changes seen as conversion of TeO_4 structural units to TeO_{3+1}/TeO_3 units. A degree of conversion of TeO_4 structural units to TeO_{3+1}/TeO_3 units could be correlated with the optical band gap changes that is with an increase in the intensity of Raman features assigned to TeO_{3+1}/TeO_3 units (715 - 804 cm^{-1}) the optical band gap increases. However, only for last two glasses significant structural changes were observed that is the intensity of Raman features related to TeO_{3+1} and/or TeO_3 units exceeds that one related to TeO_4 units.

Acknowledgements

Support from the project VZ 0021627501 is acknowledged by H. Ticha and support from the project AVOZ 40500505 is acknowledged by L. Tichy. We are indebted to Dr. M. Vlcek from Institute of Macromolecular Chemistry of the Academy of Sciences of

the Czech Republic (Joint Laboratory of Solid State Chemistry of Institute of Macromolecular Chemistry of Academy of Sciences of the Czech Republic and the University of Pardubice) for microprobe X-ray analysis.

References

[1] T. Sekiya, N. Mochida, A. Ohtsuka, M. Tonokawa J. Non-Cryst. Solids **144**, 128 (1992).
[2] M. D. Donnell, A. B. Seddon, D. Furniss, V. K. Tikhomirov, C. Rivero, M. Ramme, R. Stegman, G. Stegman, K. Richardson, R. Stolen, M. Couzi, T. Cardinal J. Amer. Cer. Soc. **90,** 1448 (2007).
[3] M. Soulis, A.P. Mirgorodsky, T. Merle-Méjan, O. Masson, P. Thomas. M. Udovic, J. Non-Cryst. Solids **354,** 143 (2008).
[4] C. Riviero, R. Stegeman, K. Richardson, G. Stegeman, G. Turri, M. Bass, P. Thomas, M. Udovic, T. Cardinal, E. Fargin, M. Couzi, H. Jain, A. Miller, J. Appl. Phys. **101,** 023526 (2007).
[5] T. Hazakawa, M. Koduka, M. Nogami, J. R. Duclere, A. P. Mirgorodsky, P. Thomas, Scripta Materialia **62**, 806 (2010) 806.
[6] J. Ozdanova, H. Ticha, L. Tichy, Adv. Mat. Res. **39-40,** 185 (2008).
[7] J. Ozdanova, H. Ticha, L. Tichy, J. Non-Cryst. Solids **353**, 2799 (2007).
[8] J. Ozdanova, H. Ticha, L. Tichy, Opt. Mater. doi:10.1016/j.optmat.2010.01.031.
[9] J. Schwarz, H. Ticha, L. Tichy, J. Optoelectron. Adv. Mater. **6**, 737(2004).
[10] K. Kotkova, H. Ticha, L. Tichy Optoelectron. and Adv. Mat.- Rapid Communications **1**, 36 (2007).
[11] E.A. Davis, N. F. Mott Philos. Mag. **22**, 903 (1970).
[12] J. I. Pankove Optical Properties in Semiconductors. Prentice-Hall, Englewood Cliffs, NJ, (1971).
[13] H. Ticha, L. Tichy, J. Optoelectron. Adv. Mater. **4,** 737 (2004).
[14] A. G. Kalampounias, G. N. Papatheodorou, S. N. Yannopoulos J. Phys. Chem. Solids **68**, 1029 (2007).
[15] M. E. Lines J. Non-Cryst. Solids **89**, 141 (1987).
[16] M. E. Lines, A. E. Miller, K. Nassau, K. B. Lyons J. Non-Cryst. Solids **89**, 163 (1987).
[17] A. E. Miller, K. Nassau, K. B. Lyons, M. E. Lines J. Non-Cryst. Solids **99**, (1988) 289.
[18] S. N. Yannopoulos, G. N. Papatheodorou, and G. Fytas Phys. Rev. B **60**, 15131 (1999).
[19] M. Maczka, J. Hanuza, J. Baran, A. Hushur, S. Kojima J. Chem. Phys. **125**, 244503 (2006).
[20] G. S. Murugan, Y. Ohishi, J. Appl. Phys. **96**, 2440 (2004).
[21] A. Aronne, V.N. Sigaev, B. Champagnon, E. Fanelli, V. Califano, L. Z. Usmanova and P. Pernice J. Non-Cryst. Solids **351**, 3610 (2005).
[22] T. Cardinal, E. Fargin, G. Le Flem, M. Couzi, L. Canioni, P. Segonds, A. Ducasse, F. Adamietz Eur. J. Solid State Inorg. Chem. **33**, 597 (1996).
[23] Handbook of Chemistry and Physics 77th Edition, (Ed.: D.R. Lide), CRC Press, Boca Raton, (1996).
[24] A. Berthereau, E. Fargin, A. Villezusanne, R. Olazcuaga, G. Le Flem and L. Ducasse J. Solid State Chem. **126**, (1996) 142.
[25] S. Akamine, T. Nanba, Y. Miura and S. Sakida in 9th Biennial Worldwide Congress on Refractories, 8-11 November, Orlando, Florida (2005).
[26] M. Udovic, P. Thomas, A. Mirgorodsky, O. Durand, M. Soulis, O. Masson, T. Merle-Mejean and J.C. Champarnaud-Mesjard J. Solid State Chem. **179**, 3252 (2006).
[27] M. Tzolov, N. Tzenov, D. Dimova-Malinovska, M. Kalitzova, C. Pizzuto, G. Vitali, G. Zollo, I. Ivanov, Thin Solid Films **396**, 276 (2001).
[28] A. N. Moiseev, A. V. Chilyasov, V. V. Dorofeev, O. A. Vostrukhin, E. M. Dianov, B. G. Plotnichenko, V. V. Koltashev, J. Optoelectron. Adv. Mater. **6**, 737 (2004).

\

*Corresponding author: ladislav.tichy@upce.cz